Indian Journal of Advances in Chemical Science

Research Article

Noval Ni (II) and Mn (II) Schiff Base Complexes Derived from 1, 1'-[benzene-1,4-diyldi(1*Z*)eth-1-yl-1-ylidene] and 2,3-diacetylhexane-2,5-dione: Fabrication, Characterization, Biological and Photocatalytic Potential

Savita Ahlawat, Anita Rani*

Department of Chemistry, School of Basic and Applied Science, IEC University, Baddi, Solan, H.P., India, 173103

ABSTRACT

Noval Schiff base ligand (BYDU-L) has been recovered by condensation reaction between 1, 1'-[benzene-1,4-diyldi(1*Z*) eth-1-yl-1-ylidene] and 2,3-diacetylhexane-2,5-dione. Moreover, new Ni (II) and Mn (II) complexes of the ligand were also synthesized by using reflux method. All the compounds were converted in powered form and characterized in detail by spectral and analytical techniques such as Fourier transform infrared spectroscopy, nuclear magnetic resonance, X-ray diffraction, and mass spectral analysis. The compounds were also found to depict excellent antimicrobial activity against different strains of microbes. The result of anti-angiogenic activity was also detected by counting number of blood cells through CAM method. The photocatalytic potential of the synthesized compounds was proved by using Congo red dye degradation at different time intervals.

Key words: Antiangiogenic activity, Antimicrobial, Metal complexes, Photocatalytic, Schiff base.

1. INTRODUCTION

The class named "Schiff bases" is regarded as a special category of ligands containing a variety of donor atoms with very interesting mode of co-ordination toward different metals [1-3]. Due to excellent co-ordination capacity, a large number of Schiff bases along with their complexes have been evaluated for various important and interesting applications like catalysis olefin hydrogenation, reversible binding of oxygen, photochromic capability, and many more [4-7]. As it is known that the identity of Schiff base is presence of azomethine linkage in the molecule, which is responsible for a number of biological activities such as antibacterial, antitumor, herbicide, antifungal, antioxidant, antiviral, antidepressant, anti-angiogenesis, antipyretic, antiproliferative, DNA-Photo cleavage, antidiabetic, and many more [3,8-14]. Some Schiff base derivatives have been found to show anti-glycation and α-glucosidase inhibition activity [15,16]. On the other hand, different derivatives of this class are being used in the form of fluorescent sensors to treat diabetic biomarker beta-hydroxybutyrate [17]. All these activities of the Schiff base are found to increase by many folds of time when ligands are subjected to co-ordination with different metals such as Cu [18], Pd [19], Mo [20], Zr [21], Ni [22], Zn [23], Ru [24], Mo [20], Mn [25], and W [26]. These complexes have been prepared through the introduction of ligand into the metal precursor in required ratio along with appropriate experimental conditions. The presence of donor atoms like N, S, P, and O are required to be present in ligand so that metal can coordinate. Among them N and S chelating ligands have attracted appreciable attention due to their tremendous Physiochemical and biological activities. Despite interesting biological activities, the Schiff base ligands are efficient in showing photocatalytic activity, when measured against particular effluent.

This research article elaborates the synthesis of noval Schiff base ligand by refluxing ethanolic solution of 1,1'-[benzene-1,4-diyldi(1*Z*)eth-1-yl-1-ylidene]diurea with 3,4-diacetylhexane-2,5-dione. The Schiff base ligand (BDUA-L) so obtained was then allowed to react with Ni (II) and Mn (II) metals to get chelates of respective metals, that is, (BDUA-L-Ni) and (BDUA-L-Mn). Further antimicrobial and anti-angiogenic activities were evaluated for the synthesized compounds. Moreover, photocatalytic activity was also measured using Congo red dye.

2. MATERIALS AND METHODS

All the solvents, reagents or chemicals used were of analytical grade purchased from Sigma-Aldrich and Merck and used as such without any purification. The melting points of all the compounds were evaluated in an open glass capillaries. The amount of purity of the Schiff base was established by thin layer chromatography on Silica gel-G plates and iodine vapors were used to visualize the spots. The elemental analysis was performed using a Perkin-Elmer elemental analyzer at SAIF Lab (Punjab University, Chandigarh, India). Vibrational spectra of all the synthesized compounds were recorded by KBr pellet method on FT-IR Shimadzu 8400S spectrophotometer, in the region 4000–400 cm^{-1} range. The Proton nuclear magnetic resonance (^{1}H NMR) and carbon-13 nuclear magnetic resonance (^{13}C-NMR) of selected compounds in DMSO-d_6 were recorded on Bruker Avance NEO 500 MHz spectrometer using Tetramethylsilane as internal standard at SAIF Lab, Chandigarh, India. X-ray diffraction (XRD) results were

***Corresponding author:**
Anita Rani
E-mail: caoudhary.anita@gmail.com

ISSN NO: 2320-0898 (p); 2320-0928 (e)
DOI: 10.22607/IJACS.2025.1302001

Received: 25th January 2025 ;
Revised: 02th February 2025;
Accepted: 10th March 2025;
Published: 02nd May 2025

done at IIT Mandi (Himachal Pradesh, India). Mass spectra were recorded on WATERS, QTOF MICROMASS (ESI-MS) at SAIF Lab (Punjab University, Chandigarh, India) to find the molecular mass of the ligand and complexes.

2.1. Synthesis of 1, 1'-[benzene-1,4-diyldi(1Z)eth-1-yl-1-ylidene] diurea

1 mole of Dimethyl tetraphthalate and 2 mole of urea were added to 40 mL of ethanol in a 100 mL round bottom flask. The content was refluxed for 4 h on a heating mentle using a water condenser. The reaction mixture was allowed to cool at room temperature for 30 min. After cooling, the solution was poured into a 200 mL beaker containing ice cubes. Off white colored precipitates obtained which were washed several times with water and finally dried in desicator overnight [Scheme 1].

2.2. Synthesis of Ligand (BYDU-L)

The Schiff base ligand (BYDU-L) was synthesized by dissolving 2 mole of 1, 1'-[benzene-1,4-diyldi(1*Z*)eth-1-yl-1-ylidene]diurea in 20 mL of hot ethanol in 100 mL round bottom flask. After formation of homogenous solution, 1 mole of 2,3-diacetylhexane-2,5-dione was added in the same flask and the content was refluxed at 80–90°C for 5 h. After being allowed to cool at room temperature, the light pale yellow product was filtered out, recrystalised and then dried under vacuum [Scheme 2]. The yield of the product was found to be 70% with melting point of 165°C.

2.2.1. Elemental analysis

Calculated (found) % for [$C_{34}H_{34}N_8O_4$]: C 66.01 (66.04); H 5.50 (5.46); N 18.12 (18.09); O 10.35 (10.32). IR (KBr, ν max, cm^{-1}): 3306 (N-H), 1704 (C=O), 1590 (C=N), 1257 (C-N). ^{1}H-NMR (600 MHz, DMSO-*d*6) TM ppm: δ 2.31 (s, 3H, -CH_3-C=N), δ 2.50 (s, 3H, -CH_3-C-Aromaic) δ 7.12-7.62 (d, 4H, aromatic ring). ^{13}C-NMR (δ, ppm): 18.50 (CH_3), 116.16–144.64 (Aromatic Carbon), 151.39 (C=N), 165.43 (C=O). (LCMS (*m/z*): calculated (found) m/z 618 (618.2145) for [$C_{34}H_{34}N_8O_4$].

2.3. Synthesis of Metal Complexes

Noval metal complexes of synthesized Schiff base ligand (BYDU-L) have been prepared in ethanol in 1:2 (Ligand: Metal) ratio. The metal salts used here were chlorides of Ni(II) and Mn (II). The content was heated on water bath for 3 hr. After that the solution was allowed to cool at room temperature. Light brown and light grey colored precipitates appeared out for (BYDU-L-Ni) and (BYDU-L-Mn) complexes, respectively [Scheme 3]. The so obtained precipitates were recrystalized and dried in vacuum desicator overnight.

2.3.1. Elemental analysis

Calculated (found) % for [$C_{34}H_{34}N_8O_4Ni_2Cl_4$]: C 46.46 (46.42); H 3.87 (3.84); N 12.77 (12.79); O 7.29 (7.25); Ni 13.38 (13.40); Cl 16.17 (16.19). IR (KBr, ν max, cm^{-1}): 3263 (N-H), 1678 (C=O), 1550 (C=N), 1236 (C-N). ^{1}H-NMR (600 MHz, DMSO-*d*6) TM ppm: δ 2.39 (s, 3H, -CH_3-C=N), δ 2.64 (s, 3H, -CH_3-C-Aromaic) δ 7.74–7.24 (d, 4H, aromatic ring). ^{13}C-NMR (δ, ppm): 18.65 (CH_3), 121.24–149.72 (Aromatic Carbon), 155.64 (C=N), 170.34 (C=O). (LCMS (*m/z*): calculated (found) m/z 877.1988 (877.201) for [$C_{34}H_{34}N_8O_4Ni_2Cl_4$].

Calculated (found) % for [$C_{34}H_{34}N_8O_4Mn_2Cl_4$]: C 46.89 (46.93); H 3.90 (3.88); N 12.87 (12.85); O 7.35 (7.38); Mn 12.62 (12.65); Cl 16.29 (16.25). IR (KBr, ν max, cm^{-1}): 3268 (N-H), 1672 (C=O), 1562

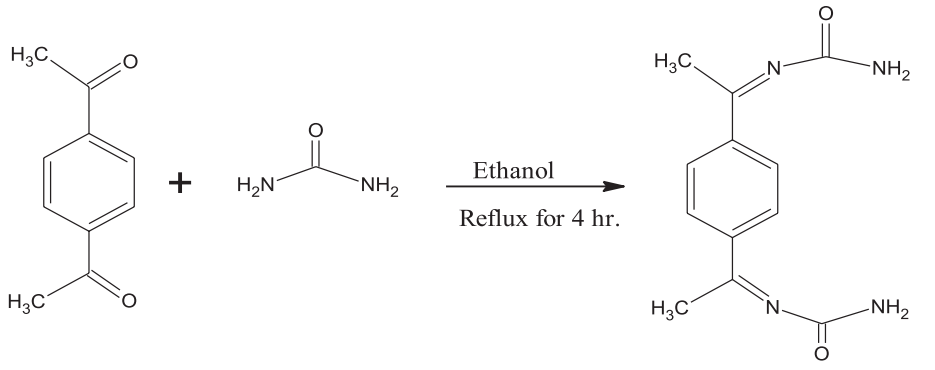

Dimethyl tetraphthalate | Urea | 1,1'-[benzene-1,4-diyldi(1Z) eth-1-yl-1-ylidene]diurea

Scheme 1: Synthesis of 1, 1'-[benzene-1,4-diyldi(1*Z*)eth-1-yl-1-ylidene]diurea.

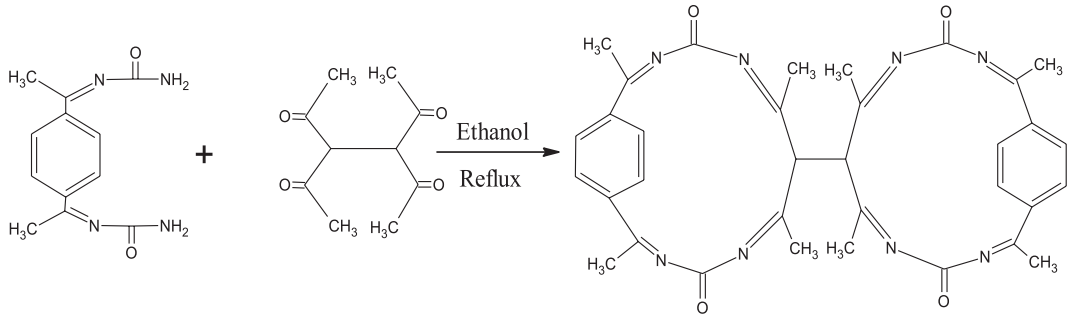

1,1'-[benzene-1,4-diyldi(1Z) eth-1-yl-1-ylidene]diurea | 3,4-diacetylhexane -2,5-dione | BYDU-L

Scheme 2: Synthesis of Schiff base ligand (BYDU-L).

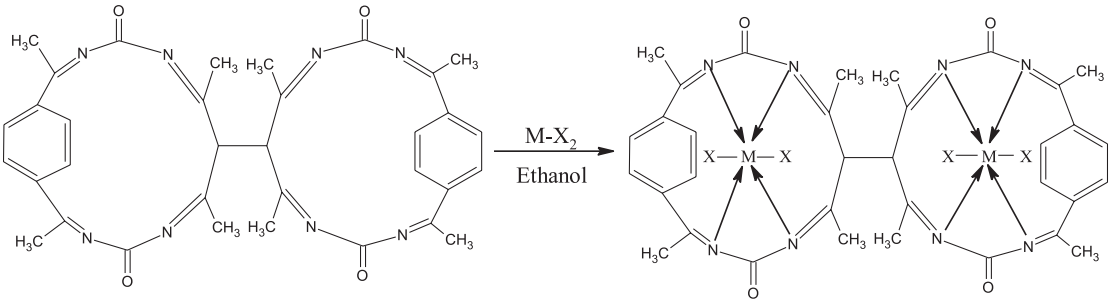

BYDU-L BYDU-L-M

Scheme 3: Synthesis of Metal complexes of Schiff base ligand BYDU-L (BYDU-L-M). Here M=Ni and Mn, X-Cl.

(C=N), 1230 (C-N). ^{1}H-NMR (600 MHz, DMSO-*d*6) TM ppm: δ 2.34 (s, 3H, -CH_3-C=N), δ 2.56 (s, 3H, -CH_3-C-Aromaic) δ 7.81–7.28 (d, 4H, aromatic ring). ^{13}C-NMR (δ, ppm): 18.60 (CH_3), 125.12–148.15 (Aromatic Carbon), 156.52 (C=N), 174.38 (C=O). (LCMS (*m/z*): calculated (found) m/z 869.68 (870.32) for [$C_{34}H_{34}N_8O_4Mn_2Cl_4$].

2.4. Biological Activities

2.4.1. Disc diffusion assay

Two different pathogenic strains of bacteria, that is, (*Escherichia coli*, *Klebsiella pneumoniae*) and fungi (*Trichophyton rubrum*, *Aspergillus niger*) were used to evaluate the *in vitro* antimicrobial activity of synthesized ligand (BYDU-L) and metal complexes. The stock solutions of ligand and its complexes, that is, 1000 ppm each was prepared in DMSO solvent. The nutrient agar and potato dextrose agar were used to prepare plates of culture medium for bacteria and fungi, respectively. Four different concentrations of all compounds (100, 200, 300, and 400 ppm) were loaded on 5 mm sterilized filter paper disk and kept on agar plates. The plates were then incubated for 24 h at 30°C so that effect of compounds could be evaluated on bacterial and fungal growth, respectively [27,28]. Fluconazole and Neomycin were taken as standard antimicrobial agents for fungal and bacterial study, respectively.

2.4.2. Chorioallantoic membrane (CAM) assay

CAM assay was used to identify the anti-angiogenic potential of the synthesized ligand (BYDU-L) and its metal complexes. The fertilized chicken eggs were treated with 70% ethanol to clean the outer surface of the eggs so that contamination and infections can be avoided. Eggs were placed in humidified chamber (70%) with a temperature range of 37°C. After that 1 mL of albumin was removed from the lower side of the eggs with the help of syringe. The pierced holes were covered with a sterilized tape. A small window was created on removing the egg shell at blunt end after 72 h of incubation. After confirming viable and normal embryo development, 0, 1, and 10 µg concentrations of the synthesized ligand and metal complexes were loaded on 5 mm sterilized filter disk and kept over the surface of CAM and placed for next 48 h under incubation. The window was again sealed with laboratory tape to avoid external contamination with the environment [29,30]. The anti-angiogenic effect of the treated compounds was manually counted in the form of branch points over CAM and calculated the percentage inhibition by using formula given below:

%Inhibition = Data of control – Data of treated × 100/Data of control

2.5. Photocatalytic Activity

Evaluation of the photocatalytic degradation was done using Congo red dye. 100 mg/L stock solution of the selected dye was prepared using distilled water. The homogenous solution was kept in dark place at room temperature. The stock solution was used to prepare different standard solutions. Similarly, the standard solutions of synthesized compounds, that is, (BYDU-L) and its metal complexes were also prepared. All the standard solutions were subjected to UV spectrophotometer to record the absorbance both before and after sunlight exposure with and without catalyst. The solutions were finally kept in the sunlight for regular interval, that is, 0, 30, 60, 90, and 120 min to get maximum absorbance of the dye. The absorbance was evaluated with the concentration of Congo red at neutral pH and concentration 10 mg/L [30]. The efficiency of photocatalysis was calculated by the formula:

$$\% \text{ Degradation } = \frac{A_0 - A_t}{A_0} \times 100$$

Here, A_0 and A_t are the absorbance of Conge Red solution before and after the photocatalysis, respectively.

3. RESULTS AND DISCUSSION

3.1. Fourier Transform Infrared Spectroscopy (FTIR)

The FTIR spectrum of the free ligand shows different characteristic bands at 3306, 1704, 1590, and 1257 cm^{-1} assignable to amine group (υ N-H) [31], carbonyl group (υ C=O) [32], azomethine linkage (υ C=N) [33], and Carbon-Nitrogen single bond (υ C–N) stretching modes, respectively [Figure 1a]. On complexation, the (υ C=N) band is shifted to lower wave number with respect to free ligand, that is, at 1550 cm^{-1}, expressing that the nitrogen of the azomethine group get coordinated to metal through co-ordination bond [Figure 1b]. Further the value for (υ C=O) in metal complex also appeared between 30 cm^{-1} and 40 cm^{-1} at lower value than the free ligand [34]. The FTIR spectra of metal chelates signify its presence with new band at 490 cm^{-1} range assigned to (M–N) that prove the indeed occurrence of complexation [35].

3.2. ^{1}H-NMR Spectra

NMR is a unique technique that helps to determine the chemical structure of tested compounds by identifying different type of protons present in it. The proton NMR spectra of the free hydrazone along with their complexes were recorded in DMSO-d6 and the attribution of the signals is presented in the Section. The spectra of Schiff base ligand shows total of four types of signals in which two distinguish peaks are in the form of singlet and a pair of doublet [Figure 2]. Among them, two singlets between 2.3145 ppm and 2.5014 ppm, corresponding to the hydrogen atoms of the methyl group directly attached to imine group and indirectly attached to benzene ring respectively. The two doublets between 7.1241 ppm and 7.6214 ppm correspond to the two environmentally different hydrogen atoms of aromatic ring [36,37]. The information obtained from the spectra coincide with the proton present in the proposed structure; hence, this prove the formation of required compound.

3.3. ^{13}C-NMR Spectra

^{13}C-NMR spectra provide evidences about the presence of number of ^{13}C atoms in the synthesized ligand and have been recorded for the ligand only. In the spectrum of the free ligand, a sharp signal at 151.39 ppm reasonably certifies the existence of azomethine carbon [Figure 3]. On the other hand, the resonance signals appeared in the region 116.16–144.64 ppm has been assigned to all the possible carbon atoms of aromatic ring in the ligand molecule [38]. Methyl carbon certifies its presence in the form of weak signal at 18.51 ppm while sharp singlet at 165.43 ppm elaborates the identity of carbonyl carbon [39].

3.4. Mass Spectra

The mass spectrum of ligand (BYDU-L) has been shown in [Figure 4]. A clear view of spectrum depicted the molecular ion peak at m/z = 686 for [$C_{34}H_{34}N_8O_4$]. The different competitive fragmentation pathways of ligand give various peaks for particular fragments, that is, m/z = 558 for [$C_{33}H_{30}N_6O_3$], m/z = 498 for [$C_{32}H_{26}N_4O_2$], m/z = 312 for [$C_{34}H_{34}N_8O_4$], and m/z = 126 for [$C_{10}H_6$] after elimination of stable fragments [Scheme 4]. The intensity of all these peaks describes the abundance and stability of resulted fragments. The mass spectra of Nickel complex of the ligand has been shown in [Figure 5]. The spectrum show a clear peak at m/z = 877, which confirm the preparation of proposed molecule with molecular formula [$C_{34}H_{32}N_4O_4Ni_2Cl_4$]. The calculated value for obtained compound coincides with the observed value and it certify the indeed occurrence of coordination.

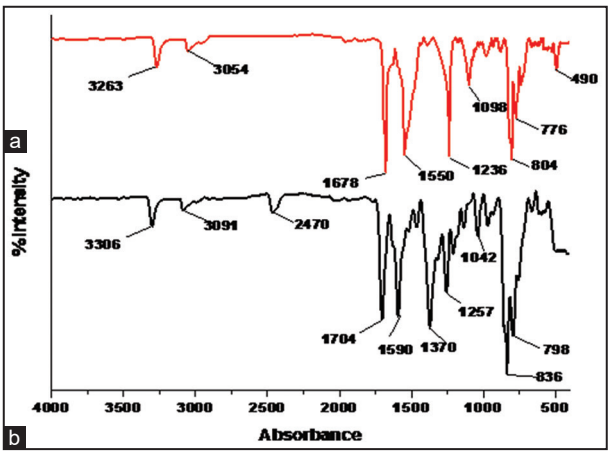

Figure 1: Fourier transform infrared spectroscopy spectra of (a) BYDU-L and (b) BYDU-L-Ni.

3.5. XRD

The visual appearance of ligand was found to be amorphous but the obtained Ni (II) and Mn (II) complexes were looked as crystalline due to presence of shiny and organized crystals. For confirmation XRD study was done for Ni (II) complex which is shown in [Figure 6]. The intensity of the peaks was recorded at an angle of 2 theta degree. A large number of sharp peaks can be seen between the ranges of 20 and 40, indicating the crystalline nature and well defined shape of the metal complex as compare to ligand alone. The increment in crystallinity on going from ligand to complex may be due to introduction of metal salt in the reaction medium and retention of metal in the core of ligand that result the formation of metal complex [40].

Grain size of the Ni complex has been measured by Scherre's formula by considering the full width at half maximum of the XRD peaks. (D= Kλ/βCos θ) Where D = Particle size, K = Dimensionless shape factor, λ = X-ray wavelength (0.15406 Å), β = full width at half maximum of the diffraction peak, θ = Diffraction angle. The crystalline size of Ni(II) complex has been found to be 24.12 nm which suggest the existence of complex in nanocrystalline phase [41].

3.6. Scanning Electron Microscopy (SEM) Analysis

The SEM technique is a type of electron microscopy that scans the surface of the targeted material and produce produces meaningful pictures by scanning its surface with the help of focused electron beam. After reacting the electron beam with sample atom, it sends out different signals that disclose the shape, surface topography, and size

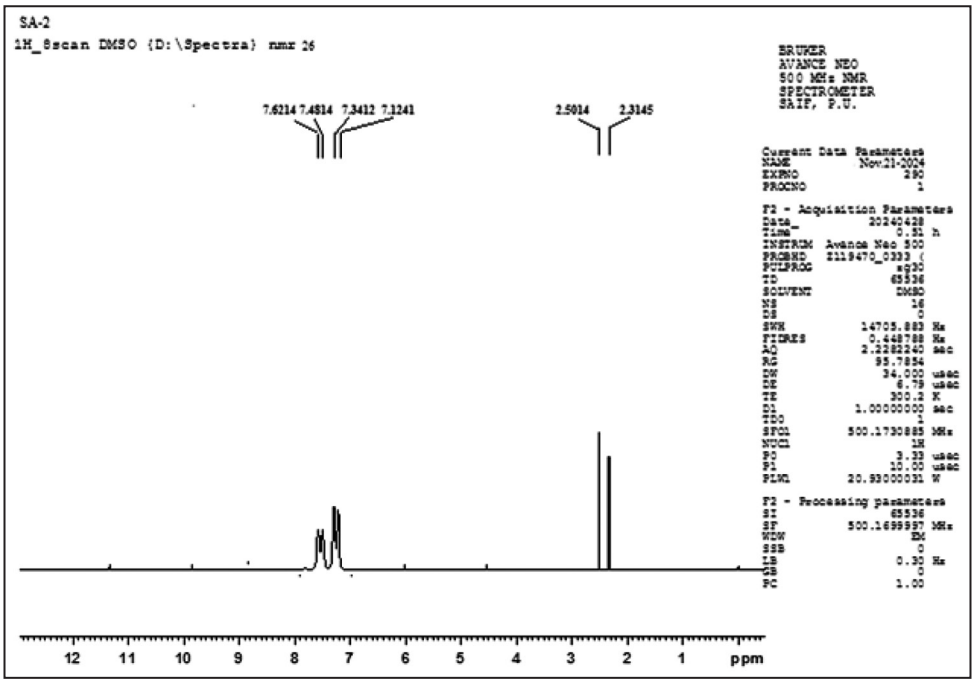

Figure 2: Proton nuclear magnetic resonance spectra of BYDU-L.

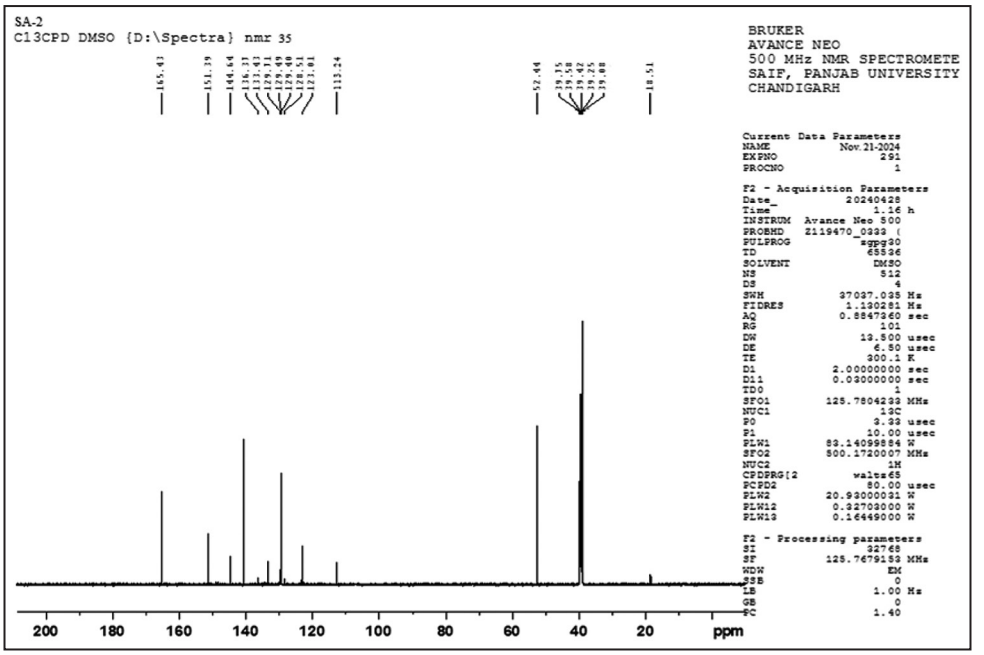

Figure 3: Carbon-13 nuclear magnetic resonance spectra of BYDU-L.

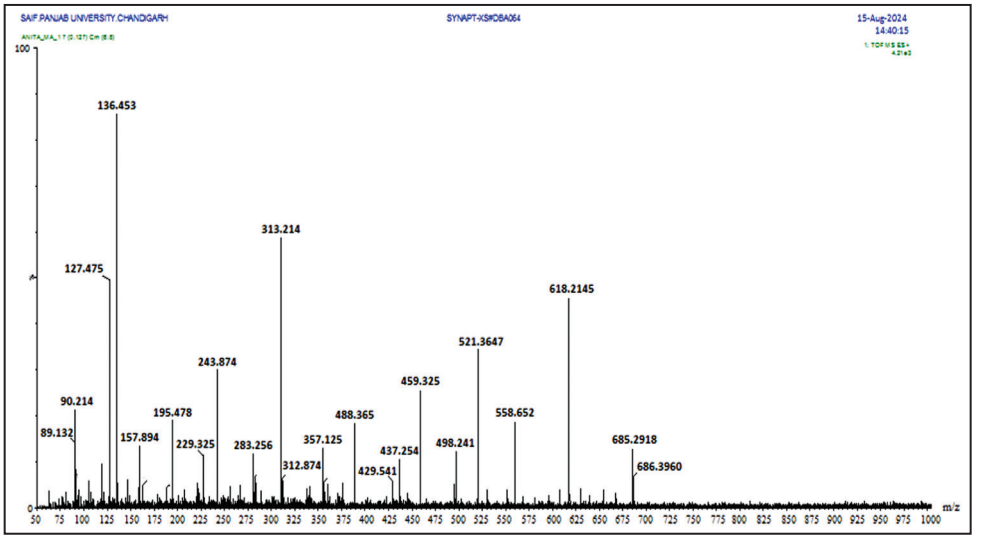

Figure 4: Mass spectra of BYDU-L.

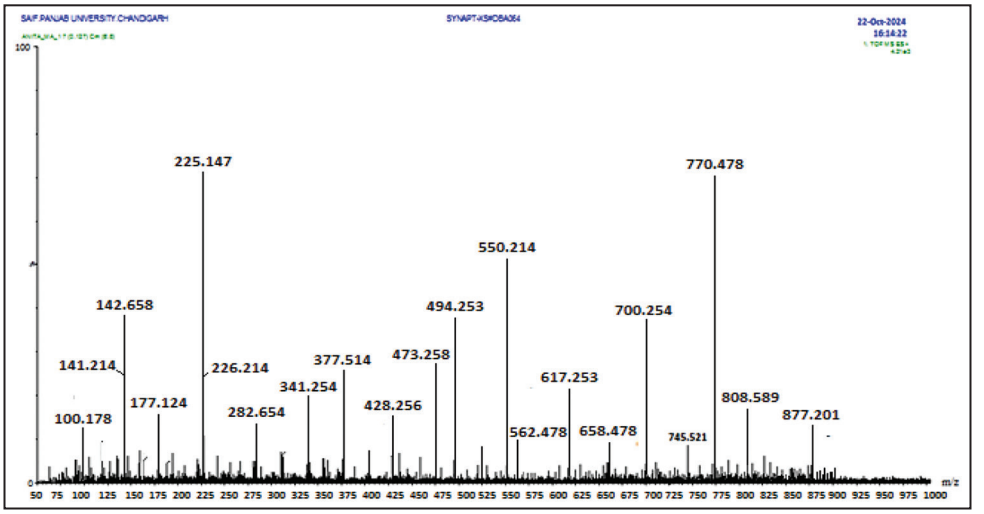

Figure 5: Mass spectra of BYDU-L-Ni.

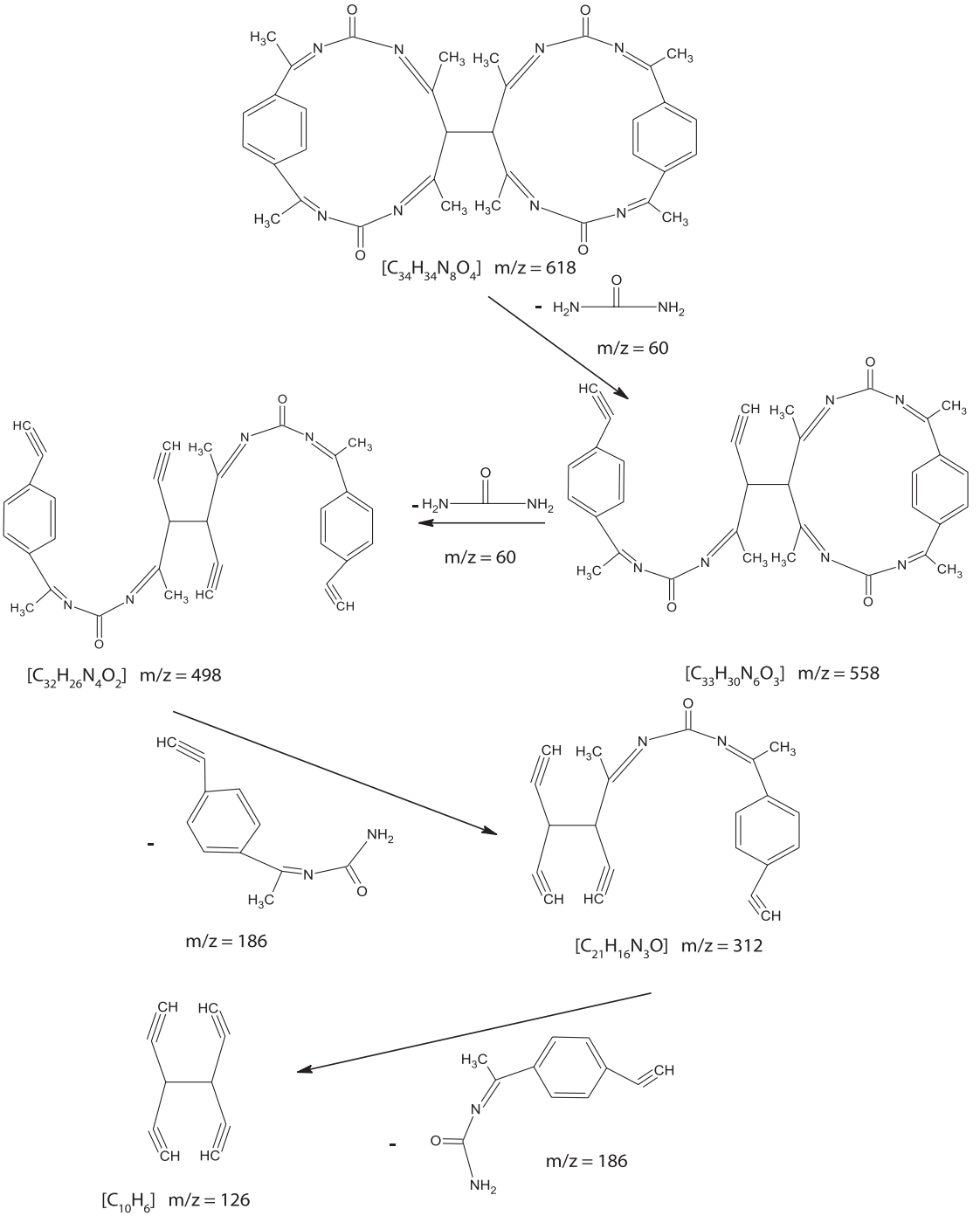

Scheme 4: Mass fragmentation pattern of BYDU-L.

of the synthesized compound. The amorphous ligand (BYDU-L) and crystalline Ni (II) complex (BYDU-L-Ni) were used to perform the SEM analysis [Figure 7]. The particles of ligand are clearly indicated overlapped and in the form of spread sheet [Figure 7a] while the image of Ni (II) complex [Figure 7b] describes the emergence of new surface after coordination of Ni (II) particles in the bulk of ligand [42].

3.7. Antimicrobial Activity

The antimicrobial screening was done by taking two strains of bacteria and two strains of fungi, that is, (*E. coli*, *K. pneumoniae*) and (*T. rubrum, A. niger*), respectively. It is important to note that all the metal chelates exhibited impressive inhibitory effects when compared with parent ligand [43,44]. The excessive activity of metal complexes can be explained on the basis of chelation theory. The Ni (II) complex found to exhibit excellent antifungal activity as compare to antibacterial. Moreover, the antimicrobial activities were found to be directly proportional to the concentration of the compounds hence increases with increasing concentration of compounds under investigation [Figure 8].

The maximum inhibition potency of (BYDU-L-Ni) for tested microorganisms is clear from [Table 1]. The zone of inhibition was found maximum, that is, between 11 mm and 23 mm with different concentrations of Ni (II) complex among all tested compounds. This suggests the maximum penetration of the same complex inside the cell membrane of microbes as compare to ligand and Mn (II) chelate.

Table 1: Results of antimicrobial activity obtained from BYDU-L, BYDU-L-Ni, and BYDU-L-Mn on the basis of zone of inhibition (mm)

Conc.	*Escherichia coli* (ppm)				*Klebsiella pneumoniae* (ppm)			
	100 (ppm)	200 (ppm)	300 (ppm)	400 (ppm)	100 (ppm)	200 (ppm)	300 (ppm)	400 (ppm)
(BYDU-L)	8 (±0.5–0.7)	12 (±0.5–0.7)	17 (±0.5–0.7)	20 (±0.5–0.7)	8 (±0.5–0.7)	11 (±0.5–0.7)	15 (±0.5–0.7)	19 (±0.5–0.7)
(BYDU-L-Ni)	11 (±0.5–0.7)	13 (±0.5–0.7)	19 (±0.5–0.7)	22 (±0.5–0.7)	12 (±0.5–0.7)	13 (±0.5–0.7)	20 (±0.5–0.7)	23 (±0.5–0.7)
(BYDU-L-Mn)	10 (±0.5–0.7)	12 (±0.5–0.7)	18 (±0.5–0.7)	21 (±0.5–0.7)	10 (±0.5–0.7)	13 (±0.5–0.7)	19 (±0.5–0.7)	21 (±0.5–0.7)
Standard	24 mm (Neomycin , 250 ppm							
Conc.	***Trichophyton rubrum* (ppm)**				***Aspergillus niger* (ppm)**			
	100 (ppm)	**200 (ppm)**	**300 (ppm)**	**400 (ppm)**	**100 (ppm)**	**200 (ppm)**	**300 (ppm)**	**400 (ppm)**
(BYDU-L)	9 (±0.5–0.7)	11 (±0.5–0.7)	17 (±0.5–0.7)	20 (±0.5–0.7)	9 (±0.5–0.7)	11 (±0.5–0.7)	16 (±0.5–0.7)	20 (±0.5–0.7)
(BYDU-L-Ni)	12 (±0.5–0.7)	14 (±0.5–0.7)	19 (±0.5–0.7)	22 (±0.5–0.7)	12 (±0.5–0.7)	15 (±0.5–0.7)	18 (±0.5–0.7)	22 (±0.5–0.7)
(BYDU-L-Mn)	10 (±0.5–0.7)	12 (±0.5–0.7)	18 (±0.5–0.7)	21 (±0.5–0.7)	11 (±0.5–0.7)	14 (±0.5–0.7)	17 (±0.5–0.7)	21 (±0.5–0.7)
Standard	24 mm (Fluconazole, 250 ppm)							

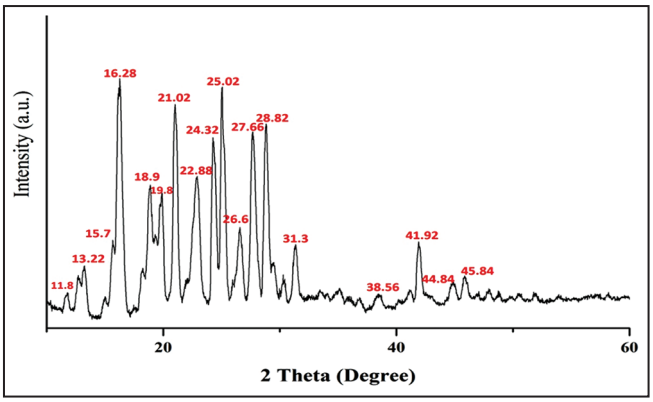

Figure 6: X-ray diffraction pattern of spectra of BYDU-L-Ni.

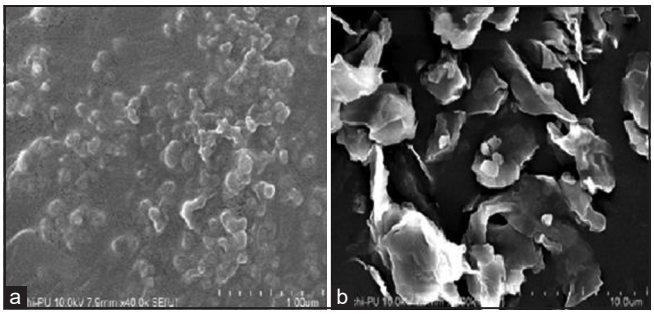

Figure 7: Scanning electron microscopy images of (a) BYDU-L and (b) BYDU-L-Ni.

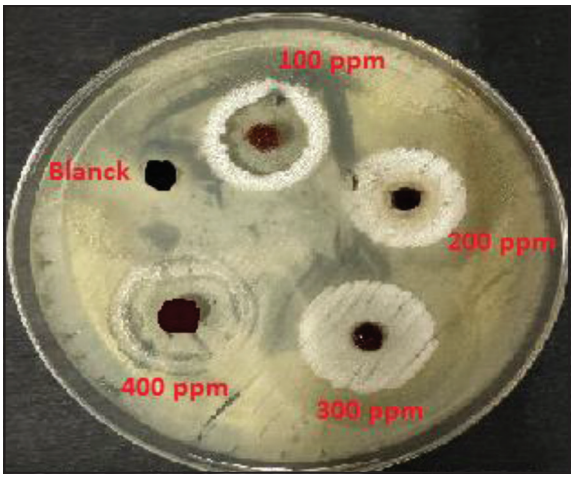

Figure 8: Antimicrobial activity shown by BYDU-L in terms of zone of inhibition (mm).

3.8. Antiangiogenic Activity

Anti-angiogenesis was performed to find the potential of newly synthesized compounds against the growth of new blood cells which is considered as a key step in the growth of tumor.

Anti-angiogenic agents are the substances that are used to treat cancer by preventing tumors from growing their own blood vessels. The enhanced anti-angiogenic activity was shown by ligand and complexes but Ni (II) complex was found inhibit the blood cell growth more effectively among all the synthesized compounds [Figure 9]. Chicken eggs were incubated with control initially which showed remarkable development of vascular sprouting after 6 h of treatment. On the other hand, Schiff base ligand produced profound inhibition to blood vessel formation after treatment. Different parameters such as vessel length, vessel size, and number of vessel branches were manually observed and compared [45,46]. The complexes of Ni and Mn were found to show the remarkable inhibition on the growth of blood vessel. Results clearly indicate that the Ni (II) complex exhibited maximum anti-angiogenic activity than Mn (II) complex.

3.9. Photocatalytic Activity

The photocatalytic efficiency of the synthesized compounds was estimated against Congo red dye at a concentration of 10 mg/L. The

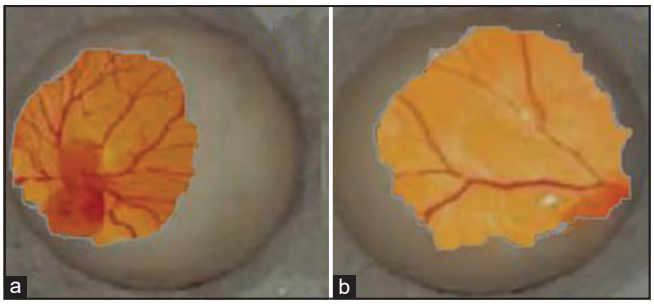

Figure 9: Antiangiogenic activity shown by (a) BYDU-L and (b) BYDU-L-Ni.

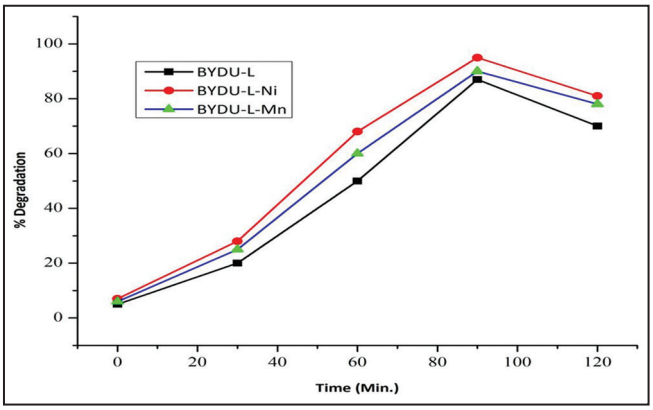

Figure 10: Result of photo degradation of Congo red dye by BYDU-L, BYDU-L-Ni and BYDU-Mn.

highest degradation of methylene blue was observed after 90 min of irradiation with solar light. The percentage degradation of ligand, Ni (II) complex and Mn (II) complex was found to be 87%, 95%, and 90%, respectively [47].

The photodegredation activity of Ni complex was found to be greatest among all the tested compounds [Figure 10]. The reason behind the increased photocatalytic efficiency of metal complexes is the separation of charges at the interface on irradiation of compounds under sunlight for a fixed limit of time which result in increment in photocatalytic activity [48]. It has been observed that the as the illumination time increases above 90 min, the Congo red dye degradation efficiency get decreases due to desorption process of the adsorbed species.

4. CONCLUSION

The Schiff base ligand (BYDU-L) have been prepared along with its two metal complexes named (BYDU-L-Ni) and (BYDU-L-Mn) by reflux method. FTIR, NMR spectroscopy, and mass spectrometry evidenced the formation of proposed compounds. XRD spectra specify the crystalline nature of the complexes as compare to ligand. All the tested compounds including ligand and metal complexes were able to show excellent antimicrobial activity but Ni (II) complex was found to show the maximum potency among all tested compounds as it was able to stop the growth of tested bacteria and fungi more effectively. The compounds were also found to show the tremendous anti-angiogenic activity. Moreover, metal complexes were able to degrade the Congo red dye more effectively than the ligand alone.

5. ACKNOWLEDGEMENT

I would like to express my gratitude to the management of IEC University and contributing author for their invaluable support in completing this research paper.

6. REFERENCES

1. B. K. Panda and A. Chakravorty, (2005) Spectroscopic properties of inorganic and organometallic compounds, ***Journal of Organometallic Chemistry***, **690:** 3169-3175.
2. K. R. Krishnapriya, and M. Kandaswamy, (2005) Coordination properties of a dicompartmental ligand with tetra- and hexadentate coordination sites towards copper(II) and nickel(II) ions Polyhedron, ***Polyhedron***, **24:** 113-120.
3. K. N. Kumar, R. Ramesh, (1999) Synthesis of lanthanide (III) complexes of chloro- and bromo-substituted 18-membered tetraazamacrocycles, ***Polyhedron***, **18:** 1561-1568.
4. D. Chen, A. E. Martell, (1987) Dioxygen affinities of synthetic cobalt Schiff base complexes, ***Inorganic Chemistry***, **26:** 1026-1987.
5. J. Collman, L. S. Hegedus, (1980) ***Principles and Application of Organotransition Metal Chemistry***, Sausalito: University Science Book.
6. J. Zhao, B. Zhao, J. Liu, W. Xu, Z. Wang, (2001) Spectroscopy study on the photochromism of Schiff bases N,N'-bis(salicylidene)-1,2-diaminoethane and N,N'-bis- (Salicylidene)-1,6-exanediamine, ***Spectrochimica Acta Part A: Molecular and Biomolecular Spectroscopy***, **57:** 149-154.
7. M. Z. Zgierski, A. Grabowska, (2000) Theoretical approach to photochromism of aromatic Schiff bases: A minimal chromophore salicylidene methylamine, ***Journal of Chemical Physics***, **113:** 7845.
8. M. Kumar, P. Siwach, H. K. Sharma, H. S. Tuli, M. Varol, A. Rani, P. Aggarwal, (2024) New schiff base derived organotin (IV) complexes: Synthesis, characterization, *in vitro* and *in silico* biological studies, ***Anti-Infective Agents***, **22(5)**: 56-68.
9. M. Kumar, Z. Abbas, P. Siwach, J. Sharma, A. Rani, S. Sharma, P. Aggarwal, P. L. Show, S. Haque, V. K. Garg, H. S. Tuli, (2023) Path of organotin complexes: Synthetic factors, mechanisms, and broad-spectrum biological influences, ***Journal of Advanced Biotechnology and Experimental Therapeutics***, **6(2)**: 386-402.
10. Z. Abbas, M. Kumar, H. S. Tuli, E.M. Janahi, S. Haque, S. Harakeh, K. Dhama, P. Aggarwal, M. Varo, A. Rani, S. Sharma, (2022) Synthesis, structural investigations, and *in vitro/in silico* bioactivities of flavonoid substituted biguanide: A novel Schiff base and its diorganotin (IV) complexes, ***Molecules***, **27(24)**: 8874.
11. D. Iacopetta, J. Ceramella, A. Catalano, C. Saturnino, M. G. Bonomo, C. Franchini, M. S. Sinicropi, (2021) Schiff bases: Interesting scaffolds with promising antitumoral properties, ***Applied Sciences,*** **11:** 1877.
12. A. Ibezim, M. N. Ofokansi, X. Ndukwe, C. S. Chiama, B.C. Obi, O.N. Isiogugu, P.E. Ikechukwu, A.M. Onwuka, S.A. Ihim, J. N. Asegbeloyin, N. J. Nwodo, (2022) Evaluation of anti-malarial potency of new pyrazole-hydrazine coupled to Schiff base derivatives, ***Malaria Journal,*** **21:** 243.
13. M. S. Tople, N. B. Patel, P. P. Patel, A. C. Purohit, I. Ahmad, H. Patel, (2023) An *in silico-in vitro* antimalarial and antimicrobial investigation of newer 7-chloroquinoline based Schiff-bases, ***Journal of Molecular Structure,*** **1271:** 134016.
14. F. S. Tokali, P. Taslimi, H. Usanmaz, M. Karaman, K. Sendil, (2021) Synthesis, characterization, biological activity and molecular docking studies of novel Schiff bases derived from thiosemicarbazide: Biochemical and computational approach, ***Journal of Molecular Structure,*** **1231:** 129666.
15. S. Daoud, S. Thiab, T. M. A. Jazzazi, T. M. A. Alshboul, S. Ullah, (2022) Evaluation and molecular modelling of bis-Schiff

base derivatives as potential leads for management of diabetes mellitus, ***Acta Pharmaceutica,*** **72:** 449-458.
16. W. Jamil, J. Shaikh, M. Yousuf, M. Taha, K. M. Khan, S. A. A. Shah, (2021) Synthesis, anti-diabetic and *in silico* QSAR analysis of flavone hydrazide Schiff base derivatives, ***Journal of Biomolecular Structure and Dynamics,*** **40:**12723-38.
17. J. Wang, N. Li, X. Q. Yang, L. L. Wang, R. Y. Ni, Y. N. He, C. Zhang, (2022) A highly selective turn-on Schiff base fluorescent sensor for diabetic biomarker beta-hydroxybutyrate (β-HB), ***Dyes Pigments,*** **207:** 110765.
18. H. Khashei Siuki, P. Ghamari Kargar, G. Bagherzade, (2022) New acetamidine Cu(II) Schiff base complex supported on magnetic nanoparticles pectin for the synthesis of triazoles using click chemistry, ***Scientific Reports,*** **12:** 3771.
19. H. Kargar, M. Fallah-Mehrjardi, R. Behjatmanesh-Ardakani, M. Bahadori, M. Moghadam, M. Ashfaq, K. S. Munawar, M. N. Tahir, (2022) Spectroscopic investigation, molecular structure, catalytic activity with computational studies of a novel Pd (II) complex incorporating unsymmetrical tetradentate Schiff base ligand, ***Inorganic Chemistry Communications,*** **142:** 109697.
20. H. Kargar, M. Nateghi-Jahromi, M. Fallah-Mehrjardi, R. Behjatmanesh-Ardakani, K. S. Munawar, S. Ali, M. Ashfaq, M. N. Tahir, (2022) Synthesis, spectral characterization, crystal structure and catalytic activity of a novel dioxomolybdenum Schiff base complex containing 4-aminobenzhydrazone ligand: A combined experimental and theoretical study, ***Journal of Molecular Structure,*** **1249:** 131645.
21. F. Ghobakhloo, D. Azarifar, M. Mohammadi, H. Keypour, H. Zeynali, (2022) Copper (II) Schiff-base complex modified UiO-66-NH_2 (Zr) metal-organic framework catalysts for Knoevenagel condensation-Michael addition-cyclization reactions, ***Inorganic Chemistry,*** **61:** 4825-4841.
22. A. Ourari, D. Aggoun, H. E. Karce, R. Berenguer, E. Morallon, T. Lanez, Y. Ouennoughi, (2022) Electrochemistry and study of indirect electrocatalytic properties of a novel organometallic Schiff base nickel(II) complex, ***Journal of Organometallic Chemistry,*** **976:** 122441.
23. H. Kargar, M. Fallah-Mehrjardi, M. Ashfaq, K. S. Munawar, M. N. Tahir, R. Behjatmanesh-Ardakani, H. A. Rudbari, A. A. Ardakani, S. Sedighi-Khavidak, (2021) Zn(II) complexes containing O,N,N,O-donor Schiff base ligands: Synthesis, crystal structures, spectral investigations, biological activities, theoretical calculations and substitution effect on structures, ***Journal of Coordination Chemistry,*** **74:** 2720-2740.
24. D. Chen, C. Han, (2022) An alkoxo-bridged dinuclear ruthenium-Schiff base complex: Synthesis, structure and catalytic reactivity, ***Inorganic Chemistry Communications,*** **142:** 109595.
25. S. A. Jasim, Y. Riadi, H. S. Majdi, U. S. Altimari, (2022) Nanomagnetic macrocyclic Schiff-base-Mn(II) complex: An efficient heterogeneous catalyst for click approach synthesis of novel β-substitued-1,2,3-triazoles, ***RSC Advances,*** **12:** 17905-17918.
26. H. Kargar, M. Moghadam, L. Shariati, N. Feizi, (2022) Novel oxo-peroxo W(VI) Schiff base complex: Synthesis, SC-XRD, spectral characterization, supporting on chloromethylated polystyrene, and catalytic oxidation of sulfides, ***Journal of the Iranian Chemical Society,*** **19:** 3067-3077.
27. Ł. Popiołek, (2017) Hydrazide–hydrazones as potential antimicrobial agents: Overview of the literature since 2010, ***Medicinal Chemistry Research***, **26:** 287-301.
28. R. P. Bakale, G. N. Naik, S. S. Machakanur, C. V. Mangannavar, I. S. Muchchandi, K. B. Gudasi, (2018) Structural characterization and antimicrobial activities of transition metal complexes of a hydrazone ligand, ***Journal of Molecular Structure***, **1154:** 92-99.
29. S. Ambika, Y. Manojkumar, S. Arunachalam, B. Gowdhami, K. K. Meenakshi Sundaram, R. V. Solomon, P. Venuvanalingam, M. A. Akbarsha, M. Sundararaman, (2019) Biomolecular interaction, anti-cancer and anti-angiogenic properties of cobalt (III) Schiff base complexes, ***Scientific Reports***, **9(1)**: 2721.
30. C. Biswas, V. Vijayan, S. J. Panda, C. S. Purohit, M. S. Kiran, R. Ghosh, (2024) Anti-cancer and anti-angiogenic activities of some synthetic Ni (II) thiosemicarbazone complexes, ***Polyhedron***, **252:** 116888.
31. A. J. Abdulghani, R. K. Hussain, (2015) Synthesis and characterization of schiff base metal complexes derived from cefotaxime with 1H-indole-2, 3-dione (Isatin) and 4-N, N-dimethyl-aminobenzaldehyde, ***Open Journal of Inorganic Chemistry***, **5(4)**: 83.
32. V. A. Shelke, S. M. Jadhav, V. R. Patharkar, S. G. Shankarwar, A. S. Munde, T. K. Chondhekar, (2012) Synthesis, spectroscopic characterization and thermal studies of some rare earth metal complexes of unsymmetrical tetradentate Schiff base ligand, ***Arabian Journal of Chemistry***, **5(4)**: 501-507.
33. G. Venkatesh, P. Vennila, S. Kaya, S. B. Ahmed, P. Sumathi, V. Siva, P. Rajendran, C. Kamal, (2024) Synthesis and spectroscopic characterization of Schiff base metal complexes, biological activity, and molecular docking studies. ***ACS Omega***, **9(7)**: 8123-8138.
34. E. N. Mainsah, S. J. Ntum, M. A. Conde, G. T. Chi, J. Raftery, P. T. Ndifon, (2019) Synthesis, characterization and crystal structure of cobalt (II) complex of a Schiff Base derived from Isoniazid and Pyridine-4-Carboxaldehyde, ***Crystal Structure Theory and Applications***, **8(4)**: 45.
35. S. Shaygan, H. Pasdar, N. Foroughifar, M. Davallo, F. Motiee, (2018) Cobalt (II) complexes with Schiff base ligands derived from terephthalaldehyde and ortho-substituted anilines: Synthesis, characterization and antibacterial activity, ***Applied Sciences***, **8(3)**: 385.
36. P. H. Santiago, M. B. Santiago, C. H. Martins, C. C. Gatto, (2020) Copper (II) and zinc (II) complexes with Hydrazone: Synthesis, crystal structure, Hirshfeld surface and antibacterial activity, ***Inorganica Chimica Acta,*** 508: 119632.
37. J. Kaur, T. Chikate, P. Bandyopadhyay, S. Basu, R. Chikate, (2020) Cu (II) complexes of hydrazones-NSAID conjugates: Synthesis, characterization and anticancer activity, ***Journal of Coordination Chemistry***, **73(23):** 3186-3202.
38. M. Shakir, S. Hanif, M. A. Sherwani, O. Mohammad, S. I. Al-Resayes, (2015) Pharmacologically significant complexes of Mn (II), Co (II), Ni (II), Cu (II) and Zn (II) of novel Schiff base ligand,(E)-N-(furan-2-yl methylene) quinolin-8-amine: Synthesis, spectral, XRD, SEM, antimicrobial, antioxidant and in vitro cytotoxic studies, ***Journal of Molecular Structure***, **1092:** 143-159.
39. C. T. Prabhakara, S. A. Patil, A. D. Kulkarni, V. H. Naik, M. Manjunatha, S. M. Kinnal, P. S. Badami, (2015) Synthesis, spectral, thermal, fluorescence, antimicrobial, anthelmintic and DNA cleavage studies of mononuclear metal chelates of bi-dentate 2H-chromene-2-one Schiff base, ***Journal of Photochemistry and Photobiology B: Biology***, **148:** 322-332.
40. T. Manjuraj, G. Krishnamurthy, Y. D. Bodke, H. B. Naik,

H. A. Kumar, (2018) Synthesis, XRD, thermal, spectroscopic studies and biological evaluation of Co (II), Ni (II) Cu (II) metal complexes derived from 2-benzimidazole, ***Journal of Molecular Structure***, **1171:** 481-487.
41. M. M. Rashad, A. M. Hassan, A. M. Nassar, N. M. Ibrahim, A. Mourtada, (2014) A new nano-structured Ni (II) Schiff base complex: synthesis, characterization, optical band gaps, and biological activity, ***Applied Physics A***, **117:** 877-890.
42. K. Gopichand, V. Mahipal, N. N. Rao, A. M. Ganai, P. V. Rao, (2023) Co (II), Ni (II), Cu (II), and Zn (II) complexes with benzothiazole schiff base ligand: Preparation, spectral characterization, DNA binding, and *in vitro* cytotoxic activities, ***Results in Chemistry,*** **5:** 100868.
43. R. Kumar, A. A. Singh, U. Kumar, P. Jain, A. K. Sharma, C. Kant, M. S. Faizi, (2023) Recent advances in synthesis of heterocyclic Schiff base transition metal complexes and their antimicrobial activities especially antibacterial and antifungal, ***Journal of Molecular Structure***, **1294:** 136346.
44. D. Dinku, T. B. Demissie, I. N. Beas, R. Eswaramoorthy, B. Abdi, T. Desalegn, (2024) Antimicrobial activities and docking studies of new Schiff base ligand and its Cu (II), Zn (II) and Ni (II) Complexes: Synthesis and Characterization, ***Inorganic Chemistry Communications***, **160:** 111903.
45. M. E. Genel, K. Adacan, S. Selvi, D. E. Kutucu, A. Uvez, E. I. Armutak, A. Sengul, E. Ulukaya, E. G. Gurevin, (2024) Apoptosis-inducing, anti-angiogenic and anti-migratory effects of a dinuclear Pd (II) complex on breast cancer: A promising novel compound, ***Microvascular Research***, **151:** 104619.
46. M. Shahriari-Khalaji, M. Sattar, R. Cao, M. Zhu, (2023) Angiogenesis, hemocompatibility and bactericidal effect of bioactive natural polymer-based bilayer adhesive skin substitute for infected burned wound healing, ***Bioactive Materials***, **29:** 177-195.
47. A. Singh, H. P. Gogoi, P. Barman, (2023) Synthesis of metal oxide nanoparticles by facile thermal decomposition of new Co (II), Ni (II), and Zn (II) Schiff base complexes-optical properties and photocatalytic degradation of methylene blue dye, ***Inorganica Chimica Acta,*** **546:** 121292.
48. P. F. Fasna, S. Sasi, T. B. Sharmila, C. J. Chandra, J. V. Antony, V. Raman, (2022) Photocatalytic remediation of methylene blue and antibacterial activity study using Schiff base-Cu complexes, ***Environmental Science and Pollution Research***, **29(36)**: 54318-54329.

****Bibliographical Sketch***

Dr. Anita is working as Assistant Professor and currently holding the position of Head of the department in the department of chemistry at IEC University, Baddi, Solan, H.P., India. Her research includes the area of inorganic chemistry and plant based nanoparticles. She has published more than 25 research articles in the same area of research and has potential to explore the research at higher level. The basic applications of her research include the synthesis of biological and environmental beneficial agents for the wellness of live hood.